

1 **Ice core chemistry database: an Antarctic compilation of** 2 **sodium and sulphate records spanning the past 2000 years.**

3 Elizabeth R. Thomas¹, Diana O. Vladimirova¹, Dieter Tetzner¹, B. Daniel Emanuelsson¹,
4 Nathan Chellman², Daniel A. Dixon³, Hugues Goosse⁴, Mackenzie M. Grieman⁵, Amy C.F.
5 King¹, Michael Sigl⁶, Danielle G Udy⁷, Tessa R. Vance⁸, Dominic A. Winski³, V. Holly L.
6 Winton⁹, Nancy A.N. Bertler^{9,10}, Akira Hori¹¹, Chavarukonam.M Laluraj¹², Joseph R.
7 McConnell², Yuko Motizuki¹³, Kazuya Takahashi¹³, Hideaki Motoyama¹⁴, Yoichi Nakai¹³,
8 Franciele Schwanck¹⁵, Jefferson Cardia Simões¹⁵, Filipe G. L. Lindau¹⁵, Mirko Severi¹⁶, Rita
9 Traversi¹⁶, Sarah Wauthy¹⁷, Cunde Xiao¹⁸, Jiao Yang¹⁹, Ellen Mosely-Thompson²⁰, Tamara
10 V. Khodzher²¹, Ludmila P. Golobokova²¹, Alexey A. Ekaykin²²

11
12 ¹Ice Dynamics and Paleoclimate, British Antarctic Survey, High Cross, Madingley Road, Cambridge,
13 CB3 0ET, UK

14 ²Division of Hydrologic Sciences, Desert Research Institute, Reno, NV, 89512, USA

15 ³Climate Change Institute, University of Maine, 5790 Bryand Global Science Center, Orono, ME,
16 04469, USA.

17 ⁴Earth and Life Institute, Universite catholique de Louvain, Place Pasteur 3, 1348 Louvain-la-Neuve,
18 Belgium

19 ⁵Department of Chemistry, Reed College, 3203 Woodstock Blvd., Portland, Oregon, 97202, USA

20 ⁶Climate and Environmental Physics (CEP), Physics Institute & Oeschger Centre for Climate Change
21 Research (OCCR), University of Bern, Sidlerstrasse 5, 3012 Bern, Switzerland

22 ⁷Institute for Marine and Antarctic Studies, University of Tasmania, 20 Castray Esplanade, Battery
23 Point TAS 7004, Australia

24 ⁸Australian Antarctic Program Partnership, Institute for Marine & Antarctic Studies, University of
25 Tasmania, Hobart, Australia

26 ⁹Antarctic Research Centre, Victoria University of Wellington, Kelburn Parade, Kelburn, Wellington
27 6021, New Zealand

28 ¹⁰National Ice Core Facility, GNS Science, 30 Gracefield Rd, Gracefield 5040, New Zealand

29 ¹¹Kitami Institute of Technology, 090-8507, Japan

30 ¹²National Centre for Polar and Ocean Research (NCPOR), Ministry of Earth Sciences, Vasco-da
31 Gama, Goa 403804, India

32 ¹³RIKEN Nishina Center for Accelerator-Based Science, 2-1 Hirosawa, Wako, Saitama 351-0198,
33 Japan

34 ¹⁴National Institute of Polar Research, Tachikawa, Tokyo 190-8518, Japan

35 ¹⁵Centro Polar e Climático, Universidade Federal do Rio Grande do Sul, Porto Alegre, 91501-970,
36 Brazil

37 ¹⁶Chemistry Dept. "Ugo Schiff", University of Florence, 50019, Sesto F.no, Florence, Italy.

38 ¹⁷Laboratoire de Glaciologie, Department Geosciences, Environnement et Societe, Universite Libre de
39 Bruxelles, 1050 Brussels, Belgium

40 ¹⁸State Key Laboratory of Earth Surface Processes and Resource Ecology, Beijing Normal University,
41 China

42 ¹⁹State Key Laboratory of Cryospheric Science, Northwest Institute of Eco-Environment and
43 Resources, Chinese Academy of Sciences, Lanzhou 730000, China

44 ²⁰Byrd Polar and Climate Research Center, The Ohio State University, 1090 Carmack Rd. Columbus
45 OH 43210 USA

46 ²¹Limnological Institute of Siberian Branch of the Russian Academy of Sciences), Irkutsk, 664033,
47 Russia

48 ²² Arctic and Antarctic Research Institute), 38 Bering st, St Petersburg, 199397, Russia

49 *Correspondence to:* Elizabeth R. Thomas (lith@bas.ac.uk)

50

51

52

53

54

55

56

57

58

59

60

61

62

63

64

65

66

67

68

69

70

71

72

73

74 **Abstract.** Changes in sea ice conditions and atmospheric circulation over the Southern Ocean play an important
75 role in modulating Antarctic climate. However, observations of both sea ice and wind conditions are limited in
76 Antarctica and the Southern Ocean, both temporally and spatially, prior to the satellite era (1970 onwards). Ice
77 core chemistry data can be used to reconstruct changes over annual, decadal, and millennial timescales. To
78 facilitate sea ice and wind reconstructions, the CLIVASH2k working group has compiled a database of two
79 species, sodium [Na⁺] and sulphate [SO₄²⁻], commonly measured ionic species. The database comprises records
80 from 105 Antarctic ice cores, containing records with a maximum age duration of 2000 years. An initial filter
81 has been applied, based on evaluation against sea ice concentration, geopotential heights (500 hPa) and surface
82 wind fields, to identify sites suitable for reconstructing past sea ice conditions, wind strength, or atmospheric
83 circulation.

84

85

86 1 Introduction

87 Changes in wind strength and atmospheric circulation, notably the positive phase of the Southern Annular Mode
88 (SAM), have been related to increased Antarctic snowfall (Thomas et al., 2017; Thomas et al., 2008; Medley
89 and Thomas, 2019) and the widespread warming in the Antarctic Peninsula (Turner et al., 2016; Thomas et al.,
90 2009) and West Antarctica during the 20th century. Contemporaneously, Antarctic sea ice is also undergoing
91 significant change. Despite model predictions of a homogeneous decline (Roach et al., 2020), total Antarctic sea
92 ice cover has increased since 1970 (Zwally et al., 2002; Turner et al., 2009). With more recent periods of abrupt
93 decline in 2016, (Meehl et al., 2016) and 2022 (Turner et al., 2022).

94 Our understanding of winds, atmospheric circulation and sea ice is hampered by both the lack of observations
95 prior to the instrumental period (~1970s onwards) and uneven spatial coverage of paleoclimate records (Jones et
96 al., 2016; Thomas et al., 2019). Data-model intercomparison and data synthesis studies have demonstrated the
97 value of large datasets in reconstructing climate and sea ice variability over decadal to centennial timescales
98 (Dalaiden et al., 2021; Fogt et al., 2022). To meet the need for Antarctic-wide, spatially dense, and
99 intercomparable atmospheric circulation and sea ice records, we propose the use of chemical species routinely
100 measured in ice cores.

101 Sodium [Na⁺], from sea salt aerosol, has been proposed as a proxy for past sea ice extent (SIE) (Severi et al.,
102 2017; Wolff et al., 2006; Winski et al., 2021; WAIS Divide Project Members., 2013). The sea salt component
103 of [Na⁺] arises from both sea ice and open water and the relationship between [Na⁺] and sea ice varies between
104 sites (Sneed et al., 2011). High winds mobilize [Na⁺] from the sea ice surface, either in frost flowers or brine-
105 soaked snow (Huang and Jaeglé, 2017; Frey et al., 2020). The [Na⁺] reaching the ice core sites is dependent on
106 both the distances from the source, either sea ice or open ocean, and the meteorological conditions (Minikin et
107 al., 1994; Rhodes et al., 2018). [Na⁺] is therefore a valuable tracer for marine-air mass advection and changes in
108 atmospheric circulation (Dixon et al., 2004; Mayewski et al., 2017).

109 Sulphate [SO₄²⁻] is formed in the atmosphere as secondary aerosol following volcanic and anthropogenic
110 sulphur dioxide [SO₂] gas emissions. [SO₄²⁻], together with methane sulphonic acid [MSA], is the main
111 atmospheric sulphur compound formed from ocean-derived dimethylsulphide (DMS) (Gondwe et al., 2003). In
112 the southern hemisphere, marine biogenic emissions dominate the total sulphur budget (Delmas et al., 1982;
113 Legrand and Mayewski, 1997; McCoy et al., 2015). Sulphur can significantly impact cloud albedo and new
114 particle formation (Brean et al., 2021). The sea salt fraction of [SO₄²⁻] is largest at coastal and low elevation sites
115 (Dixon et al., 2004). The non-sea salt fraction, also referred to as excess [SO₄²⁻] (hereafter referred to as xs
116 [SO₄²⁻]), can be estimated based on the relationship with [Na⁺] (e.g., xs [SO₄²⁻] = [SO₄²⁻] - 0.25[Na⁺]) (O'Brien et
117 al., 1995). Excess [SO₄²⁻] has been shown to correlate with SIE at some ice core sites (Dixon et al., 2004; Sneed
118 et al., 2011). The background xs [SO₄²⁻] source, from marine biogenic deposition, is superimposed by sporadic
119 volcanic deposition of [SO₄²⁻] providing an excellent reference horizon for dating Antarctic ice cores (Dixon et
120 al., 2004; Sigl et al., 2014; Plummer et al., 2012). At low elevation and coastal sites, where background biogenic
121 sources are high, it is not always possible to identify volcanic peaks (Emanuelsson et al., 2022; Tetzner et al.,
122 2021b). In this study, [SO₄²⁻] provides a dual function: 1) as a potential proxy for SIE and 2) as a stratigraphic
123 age marker to validate submitted age-scales and subsequently align ice-core chronologies onto a common
124 chronology.

125 **1.1. The CLIVASH2k chemistry database.**

126 CLIVASH2k (CLimate Variability in Antarctica and the Southern Hemisphere over the past 2000 years) is a
127 project of the Past Global Changes (PAGES) 2k network. The CLIVASH2k database is the latest in a series of
128 community-led paleoclimate data synthesis efforts endorsed by PAGES (Kaufman et al., 2020; McGregor et al.,
129 2015; McKay and Kaufman, 2014; Tierney et al., 2015; Thomas et al., 2017; Stenni et al., 2017; Konecky et al.,
130 2020). The aim of this study is to focus on two primary species, sodium, and sulphate, as they are routinely
131 measured in ice cores and have potential links with either sea ice or atmospheric circulation. The time window
132 of the last 2000 years has been selected to cover both natural and anthropogenic changes.

133 Two main features distinguish the CLIVASH2k data compilation from previous PAGES synthesis: 1) the data
134 included are not limited to previously published records, and 2) the data comprise two distinct chemical species
135 which do not have a well-established relationship with climate. This differs from previous compilations where
136 the data can be either directly, or indirectly, compared with a modelled or observed climate parameter e.g.,
137 temperature (Stenni et al., 2017) .

138 Calls for participation in CLIVASH2k activities were widely distributed, ensuring a cross section of scientists
139 from various disciplines, geographic regions, and career stage. The targeted species to target and the selection
140 criteria were decided at several open discussion stages, followed by updates to the CLIVASH2k mailing list and
141 distributed via PAGES monthly updates.

142 **2. Methods**

143

144 **2.1. Resolution and duration.**

145 The target time-period for the database is the last 2000 years. Records of any duration could be submitted within
146 this time-period. These records could be from snow-pits and firn cores, spanning just a few seasons to years.
147 Data were requested at the highest resolution available and converted to annual averages (January – December).

148

149 **2.2. Age-scales.**

150 Most records within this time-period have been annually dated, based on the seasonal deposition of distinct
151 chemical species (including sodium, sulphate, and sulphur). The longer records, those spanning the last 500-
152 2000 years, have been synchronized previously (Sigl et al., 2014) or within this project on the WD2014 age-
153 scale (Sigl et al., 2016) or have age-scales that are broadly consistent with WD2014 (Plummer et al., 2012). This
154 new chronology is constrained by the 774 CE cosmogenic (i.e., ^{10}Be) anomaly, and is consistent with
155 dendrochronology (Büntgen et al., 2018) and ice core chronologies from Greenland (Sigl et al., 2015). The
156 WD2014 age-scale is recommended because it is consistent with the forcings applied in PMIP4/CMIP6 model
157 simulations (Jungclauss et al., 2017). Age transfer functions can now be linked to other PAGES2k
158 reconstructions and individual ice cores. There are a few exceptions. Plateau Remote and DT401, both very low
159 accumulation sites in the interior of East Antarctica, have been dated using $[\text{SO}_4^{2-}]$ (Ren et al., 2010), however,
160 the reference horizons differ from WD2014 age-scale prior to 1000 AD and cannot be confidently synchronized.
161 Another exception is partly unpublished data from the Vostok vicinity, which were dated using the snow
162 accumulation rate and volcanic age markers (this study and (Ekaykin et al., 2014).

163

164 **2.3. Peer review and publications.**

165 Unlike previous PAGES 2k compilations, the CLIVASH2k database was not constrained by the need for
166 records to be published and peer reviewed. This decision arose based on the limited number of published
167 chemistry records available and the desire to maximise the records. Published records were submitted along
168 with their original citation; unpublished records were listed as “This study”, with the data contributor included
169 as a co-author.

170

171 **2.4. Analytical methods.**

172 Both the ionic and elemental forms of sodium ($[\text{Na}]$ and $[\text{Na}^+]$) and sulphur ($[\text{S}]$ and $[\text{SO}_4^{2-}]$), respectively, were
173 accepted as part of the CLIVASH2k data call. Several analytical techniques are used to measure $[\text{Na}^+]$, $[\text{S}]$ and
174 $[\text{SO}_4^{2-}]$ in ice cores. Ionic $[\text{Na}^+]$ and $[\text{SO}_4^{2-}]$ are typically measured by ion chromatography (IC), while elemental
175 Na and S are generally measured by inductively coupled plasma mass spectrometry (ICP-MS). Unlike IC, which

176 measures the soluble fraction, ICP-MS techniques measure the total elemental concentration of both the
 177 dissolved and particulate fraction of the element. However, we note that there are different protocols for
 178 acidifying the samples prior to analysis which may result in different absolute concentrations, including the
 179 choice of acid, the acid concentration, and the acidification time. While continuous ICP-MS measurements of
 180 certain species may require correction for under-recovery, Na and S are typically fully recovered during
 181 continuous measurements (Arienzo et al., 2019). Previous comparisons of analytical methods show excellent
 182 agreement of [Na] in ice cores measured using IC and ICP-MS methods e.g., (Grieman et al., 2022). This
 183 agreement suggests that the ionic and elemental forms reported in the database can be directly compared.

184
 185 Biogenic atmospheric emissions of organic [S] species, mainly dimethyl sulfide (DMS), are a major contributor
 186 to the [S] in the Antarctic snow (Legrand and Mayewski, 1997). In the marine atmosphere DMS is oxidized to
 187 [MSA⁻] and [SO₄²⁻], which are eventually deposited on the polar ice sheets (Barnes et al., 2006). The ICP-MS
 188 technique measures total [S] in ice cores, which includes [S] contained [MSA⁻]. In contrast, the IC technique
 189 solely quantifies [S]. If total [S] and [MSA⁻] are both analysed on the same ice core, the [MSA⁻] contribution
 190 can be subtracted (Cole-Dai et al., 2021). However, continuous [MSA⁻] measurements are scarce over Antarctica
 191 (Thomas et al., 2019) and the long-term variability of both [MSA⁻] and [SO₄²⁻] is very small during the common
 192 era (Legrand et al., 1992; Saltzman et al., 2006). Thus, we applied a consistent transformation across all sites.
 193 We multiplied elemental [S] (32 g mol⁻¹) from ICP-MS measurements with three to convert to the equivalent
 194 [SO₄²⁻] (96 g mol⁻¹) without applying corrections for MSA contributions. To aid ease of comparison, all [S] has
 195 been converted to [SO₄²⁻], in the database and will be referred to only as [SO₄²⁻] in the data description.

196 2.5. Flux vs concentration.

197 [Na⁺] and [SO₄²⁻] in ice cores are generally reported as a concentration. Concentration can be converted to a
 198 deposition flux, provided that the snow accumulation rate is known. Flux (*f* in ppb kg m⁻²) is calculated
 199 according to Eq (1) and (2) for [Na⁺] and [SO₄²⁻] respectively.

$$200$$

$$201 f_{Na^+} = [Na^+] \times a \quad (1)$$

$$202$$

$$203 f_{SO_4^{2-}} = [SO_4^{2-}] \times a \quad (2)$$

204
 205 Where [Na⁺] and [SO₄²⁻] is the concentration in units of ppb and *a* is the snow accumulation in units of kg m⁻².
 206 Snow accumulation records were extracted from the Antarctic regional snow accumulation composites available
 207 at the UK Polar data centre (Thomas, 2017). The CLIVASH2k database includes both concentrations and
 208 fluxes, when available. Flux estimates from ice cores combine both wet and dry deposition, of which the
 209 contribution of these two depositional modes varies across Antarctica with elevation and distance from the
 210 source (Wolff, 2012).

212 213 2.6. Establishing the sea salt and non-sea salt component.

214 There are various methods of calculating the sea salt (ss) and excess (xs) components of an ice core chemistry
 215 record. The most-common method, as mentioned above, is to assume 100% of the [Na⁺] comes from the ocean.
 216 Then [Na⁺] can be treated as a marine reference species and the ss fraction of all other chemical species can be
 217 calculated based upon a mean ocean water elemental abundance reference value (e.g., (Lide, 2005)). If [Na⁺] is
 218 suspected of not being of marine origin, alternative methods of calculating the ss chemical fraction may be
 219 employed. For example, one may apply a standard sea-water ratio of 30.61 [Na⁺], 1.1 [K⁺], 3.69 [Mg²⁺], 1.16
 220 [Ca²⁺], 55.04 [Cl⁻] and 7.68 [SO₄²⁻] to the ion concentrations in each sample (Holland, 1978). Several studies
 221 have shown that frost flowers are depleted in [SO₄²⁻] relative to [Na⁺]. This produces a ssSO₄²⁻ value which is
 222 slightly higher than it should be for sites near the coast (Rankin et al., 2002; Rankin et al., 2000). Unfortunately,
 223 not all studies accurately measure a wide suite of chemical species. Therefore, in this study we have assumed
 224 [Na⁺] to be the primary marine species and calculated xs [SO₄²⁻] according to Eq (3) (O'Brien et al., 1995).

$$225 xs [SO_4^{2-}] = [SO_4^{2-}] - (0.25 \times [Na^+]) \quad (3)$$

226 Other ratios may be more suitable for coastal sites (Dixon et al., 2004), but for consistency we have applied the
 227 same ratio to all records reported in the database.

228

229 2.7. Data validation and recommendations

230 The two main uncertainties in the data presented arise from 1) chronological controls and 2) analytical errors.
231 As discussed in section 2.2, all records have been synchronised to a common age-scale (WD2014). Thus, when
232 using the entire database, we recommend using an error estimate of ± 2 years, for records younger than 500
233 years, increasing to a conservative error estimate of ± 5 years for records extending to 2000 years. This is the
234 maximum uncertainty estimate for the WD2014 age-scale at 2,500 years (Sigl et al., 2015). However, we note
235 that for individual records in this database the published error estimates are as low as ± 1 year (e.g., Emanuelsson
236 et al., 2022). When using individual records we recommend using the published error estimate for that record.

237 Analytical precision varies between instruments and laboratories. We recommend applying a 1 standard error
238 (σ) to the data to account for analytical errors.

239 The $[\text{Na}^+]$ and $[\text{SO}_4^{2-}]$ data is an accurate representation of either concentration or flux at a certain site.
240 However, how this relates to regional deposition is not well constrained. While we can account for the
241 uncertainty in analytical precision and dating error, we cannot define the signal to noise ratio associated with
242 small scale post-depositional process. For example, wind redistribution or the impact of local orography. The
243 regional climate and signal to local noise has been investigated for stable water isotopes in Antarctica (Münch
244 and Laepple, 2018), however, a detailed investigation of $[\text{Na}^+]$ and $[\text{SO}_4^{2-}]$ is lacking. One of the main
245 limitations, which this database will address, has been the lack of available data. We thus encourage database
246 users to investigate the regional signal by averaging records to reduce the signal to noise ratio. In this case, we
247 recommend using the standard error propagation procedure for averaging for example the square root of the sum
248 of variances of individual records divided by the number of the records.

249 Ice cores provide the only record of $[\text{Na}^+]$ and $[\text{SO}_4^{2-}]$ deposition in Antarctica, and therefore, validation against
250 reference datasets is also not possible. While progress has been made using chemical transport models to
251 represent the deposition of sea salts in Greenland (Rhodes et al., 2018), the period examined is very short
252 (annual to decadal) and has currently not been applied to Antarctica. This database will provide much needed
253 data for any future model validation. However, currently it means there are no independent data products to
254 validate our $[\text{Na}^+]$ and $[\text{SO}_4^{2-}]$ records against.

255

256 3. Data records

257 A total of 117 records were submitted, representing 105 individual ice core sites (Fig. 1). In some locations,
258 duplicate analysis or updated versions were submitted (e.g., EPICA Dome C). This includes sites where analysis
259 was undertaken at different laboratories, using different instrumentation (e.g., IC and ICP-MS) or different
260 depth resolution. Some ice cores only provide data for a single species and not all records contain both flux and
261 concentration. A total of 94 ice core sites are included in the database which provide $[\text{Na}^+]$, $[\text{SO}_4^{2-}]$ and xs $[\text{SO}_4^{2-}]$.
262 All submitted records have been included in the database. The number of records submitted is summarised in
263 Table 1. The full list of records, their location, elevation, duration, and reference are presented in appendix A
264 (Table S1).

265

266

267 **Table 1.** Summary of records submitted to the CLIVASH2k database. Combined records indicate sites which
268 contain all three species $[\text{Na}^+]$, $[\text{SO}_4^{2-}]$ and xs $[\text{SO}_4^{2-}]$.

269

	Records submitted	Analytical replicates	Number of ice cores
Total records	117	12	105
Combined	97	3	94
$[\text{Na}^+]$	106	10	96
Na^+ flux	67	3	64
$[\text{SO}_4^{2-}]$	103	6	97
SO_4^{2-} flux	64	3	61

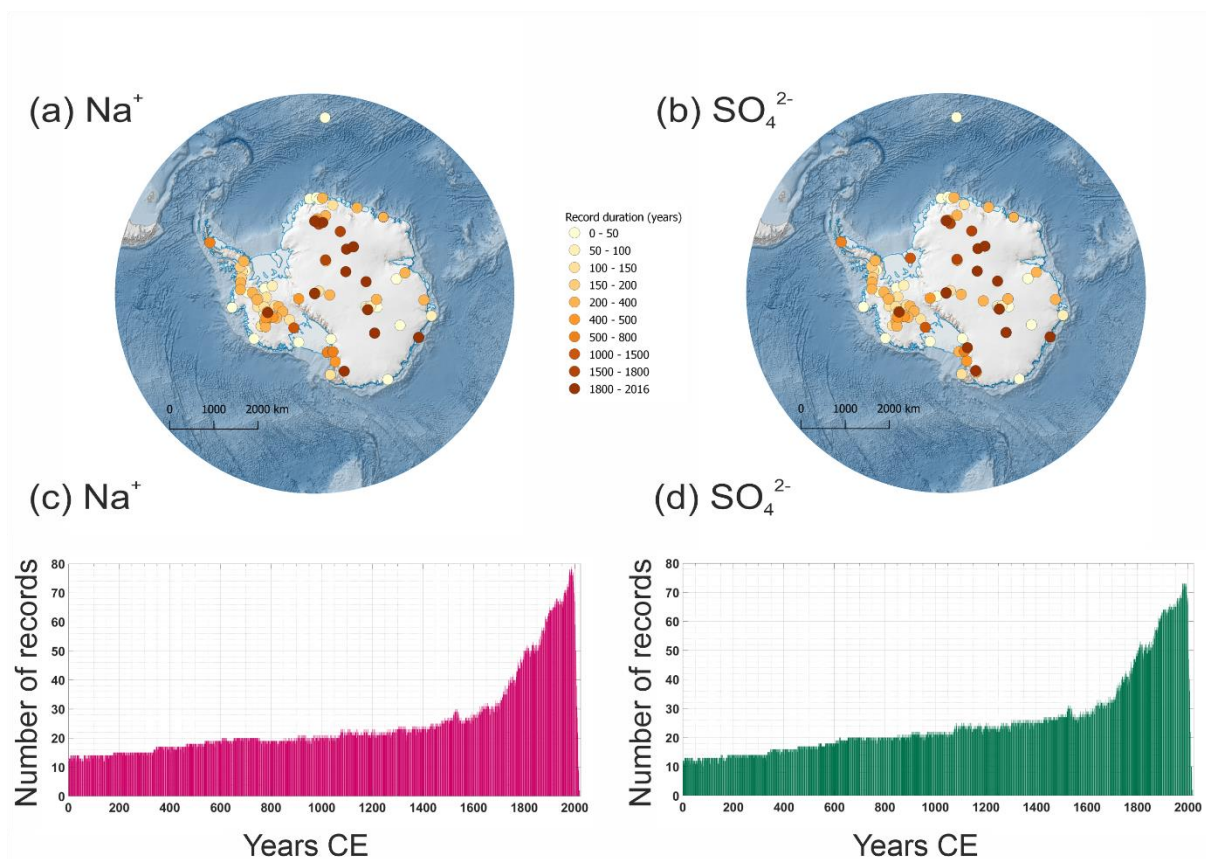
xs [SO ₄ ²⁻]	97	3	94
xs SO ₄ ²⁻ flux	61	0	61

270
271
272

3.1. Geographical and temporal coverage.

273 There is reasonable spatial coverage across Antarctica, with the largest density of records in West Antarctica
274 (Figs. 1a & 1b). In East Antarctica, notable data voids include Coats Land, Enderby and Kemp Land, Wilkes
275 Land and Terra Adelie. There is a notable absence of long records from the Antarctic Peninsula. Despite the
276 high density of records in West Antarctica, high snow accumulation in this region results in most of these
277 records only spanning the last few decades or centuries.

278 The longer duration records (>1000 years) are predominantly found on the central East Antarctic plateau, while
279 most higher snow accumulation coastal sites cover shorter timescales (Figs. 1a & 1b). The most recent year in
280 the record peaks in the late 1990s, when the highest number of cores were drilled (Figs. 1c & 1d). Only eleven
281 records span the full 2000 years.



282

283 **Figure 1.** Spatial and temporal coverage of records in the CLIVASH2k database. Map of ice core locations with
284 (a) [Na⁺], and (b) [SO₄²⁻] records. Colour coded based on record duration (number of years). The number of (c)
285 [Na⁺] and (d) [SO₄²⁻] records as a function of the years (CE) covered.

286

3.1.1. Technical validation

288 To facilitate the scientific usability of this database, we have evaluated each record in terms of its relationship
289 with key climate parameters during the observational period (1979- 2019). Given their varying temporal ranges
290 (Fig. 1), not all the records span the full satellite period. Thus, correlations are based on the largest number of
291 years available within this period. Although the database includes short records, for the data interpretation step,
292 we have only included records that have at least ten years of overlap with the satellite and reanalysis climate
293 data. Duplicate records (including updated versions and different analytical approaches) are included in the data
294 interpretation step and interpreted as individual records.

295 The objective of this climatological comparison is to provide a first level filter for the database. Based on the
296 published literature (section 1) the deposition of $[Na^+]$ and $[SO_4^{2-}]$ has been linked to changes in sea ice, winds,
297 and atmospheric circulation. Thus, these parameters have been chosen for the initial evaluation step.

298 All of the records were also correlated using ERA5 meteorological parameters (Hersbach et al., 2020), the fifth
299 generation European Centre for Medium Range Weather Forecast (ECMWF) atmospheric reanalysis data. These
300 parameters include 500-hPa geopotential height (Z500), meridional winds (v) and zonal winds (u) both at the
301 850-hPa level. The 850 hPa level was chosen to represent surface winds (relevant for sea ice reconstructions),
302 while the 500 hPa was chosen to capture larger-scale circulation across both high and low elevation sites. All
303 correlations were performed on de-trended annual average data (January – December) to correspond with the
304 annually-resolved ice core records and corrected for autocorrelation. All of the records were correlated with SIC
305 from the National Snow and Ice Data Centre (NSIDC) Nimbus-7 SMMR and DMSP SSM/I-SSMIS Passive
306 Microwave Data version 1 (Cavalieri et al., 1997).

307

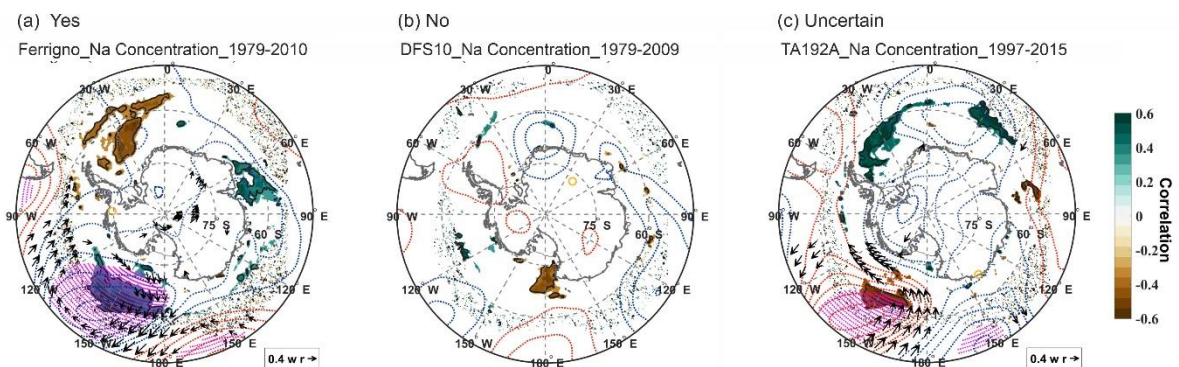
308

309 4. Data interpretation

310 4.1. Identifying sites that correlate with sea ice and atmospheric circulation

311 An example of the data interpretation output is presented in Figure 2. For consistency, correlations were
312 performed with climate variables across all longitudes in the southern hemisphere south of 50°S. This approach
313 has the potential to generate spurious results or correlations in regions that are physically unrelated to the site
314 (e.g., Fig. 2b). Indeed, studies have shown that climatic fields inherit patterns and correlations which can result
315 in statistically significant correlations by chance (Livezey and Chen, 1983). In the following sections, we only
316 refer to records that exhibited a correlation that is statistically significant at the 5% level ($p < 0.05$) (hereafter
317 referred to as significant).

318



319

320 **Figure 2.** Example correlation plots evaluated by the data interpretation team. (a) Yes example, correlation
321 observed between all three parameters. (b) No example, no significant correlation observed with any parameters.
322 In this example, a significant correlation with SIC at a distant location is likely an auto-correlation artefact. (c)
323 Uncertain example, the transport mechanism could not be verified based on the parameters of this first pass
324 filter. Yellow open circle indicates ice core location. Coloured shading indicates positive (green) and negative
325 (brown) correlations with SIC (data from NSIDC), solid black line correlations significant at the 5% level.
326 Correlations with winds (arrows) composed of u850 and v850 (ERA 5). Dashed red and blue contours represent
327 positive (red) and negative (blue) correlations with geopotential height at 500 hPa (ERA5), pink hatching is
328 significant at the 5% level. Plot titles labelled as “Site name_species_years for correlation”.

329

330 Sites identified as having a relationship with either SIC, atmospheric pressure (z500) or winds (u850 or v850),
331 had to be supported by a plausible transport mechanism or source region. Therefore, each record was
332 individually evaluated. Sites with a plausible connection were marked as “yes”, while sites which did not have a

333 plausible mechanism were marked as “no”. In the case of the Ferrigno ice core (Fig. 2a), [Na⁺] is significantly
 334 correlated with SIC is in the adjacent ocean (Amundsen-Ross Sea), and with low pressure anomalies and winds
 335 over in the Ross Sea which transport air-masses in a clockwise direction from the source region to the ice core
 336 site. Thus, for Ferrigno a plausible source region and transport mechanism has been identified. Conversely, Na
 337 at the DFS10 site is also correlated with SIC in the Ross Sea, despite the ice core being located on the opposite
 338 side of the continent (Fig. 2b). However, DFS10 [Na⁺] is not significant correlated with either atmospheric
 339 pressure or winds that could transport [Na⁺] from the Ross Sea to the ice core location. Thus, for DFS10 a
 340 plausible source region and transport mechanism has not been identified.

341

342 We have not applied a uniform cut-off size for the area of correlation or specified a minimum or maximum
 343 distance from the source region, as these features will be site specific. For example, the typical air-parcel origin
 344 height and residence time over the ice sheet is related to the site topography. As such, air parcels reaching low
 345 elevation coastal sites will originate from low elevation sources (e.g., < 2000 m) and have short residence times
 346 over the ice sheet (< 20 hours) (Suzuki et al., 2013). Some coastal sites (e.g., Sherman Island) may also be
 347 influenced by local orography (mountains), which block air-mass transport and limit the geographical extent of
 348 the [Na⁺] or [SO₄²⁻] source region e.g., Tetzner et al., 2022. Conversely, air-parcels reaching central Antarctic
 349 sites (e.g., South Pole) may originate from elevations in excess of 4000 m, and reside over the ice sheet for more
 350 than 120 hours (Suzuki et al., 2013). Thus, higher elevation sites might be influenced by long-range air-mass
 351 transport and capture changes in sea ice from relatively distant source regions e.g., Winski et al., 2021.

352

353 The database contains more concentration records than flux records. Thus, in the data interpretation we
 354 presented both the total number of sites, and the proportion of sites, that exhibit a significant correlation with
 355 meteorological parameters. The total number of eligible records for each species is shown in Table 3. The
 356 spatial distribution of records is presented in Figures 3, 4 and 5.

357

358 **Table 3.** Summary of the number of records that display a significant correlation (5% level) with SIC, wind
 359 fields (meridional (v850) and zonal (u850)), and geopotential height (z500). The total records available for the
 360 data interpretation step is shown for each species. This includes all records with more than 10-years overlap
 361 with the instrumental period (1979-2018) and includes duplicates. Brackets indicate the number of sites marked
 362 as “uncertain”. The percentage of records shown in italics underneath to account for the varying sample size.

363

Variable	[Na ⁺]	Na ⁺ Flux	[SO ₄ ²⁻]	SO ₄ ²⁻ Flux	xs [SO ₄ ²⁻]	xs SO ₄ ²⁻ Flux
Total records	88	65	84	61	81	59
SIC	69 (6) <i>78 %</i>	56 (4) <i>86 %</i>	60 (6) <i>71 %</i>	40 (5) <i>66 %</i>	68 (5) <i>84 %</i>	42 (2) <i>71 %</i>
Wind (v850 or u850)	63 (3) <i>72 %</i>	48 (4) <i>74 %</i>	54 (8) <i>64 %</i>	39 (3) <i>64 %</i>	56 (3) <i>69 %</i>	40 (3) <i>68 %</i>
Geopotential Height (z500)	47 (2) <i>53 %</i>	43 (3) <i>66 %</i>	38 (6) <i>45 %</i>	26 (3) <i>43 %</i>	40 (6) <i>49 %</i>	23 (3) <i>39 %</i>

364

365

366 4.2. Sodium (concentration and flux)

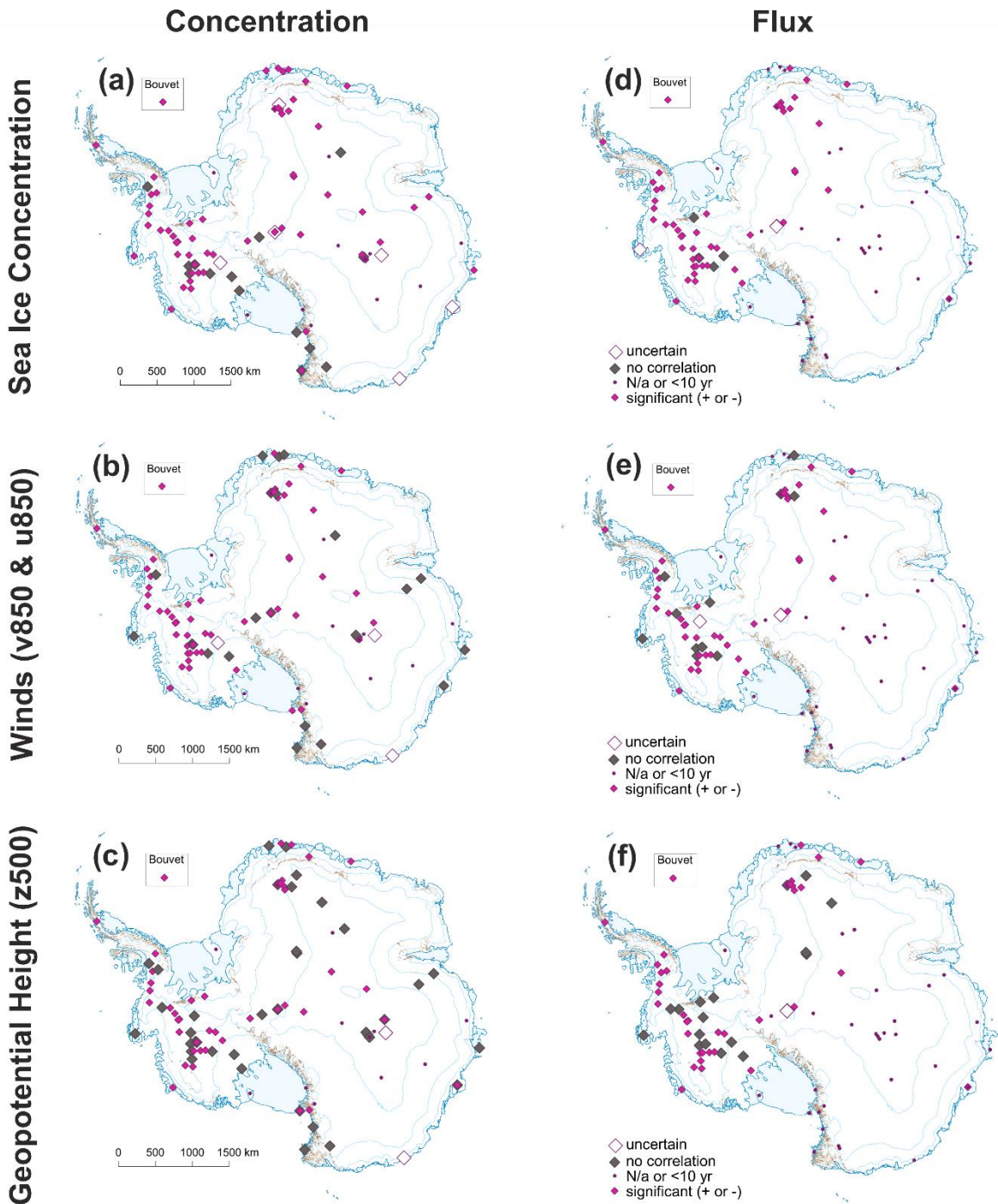
367 A total of 69 (out of 88) [Na⁺] sites exhibit a correlation with SIC, with an additional six records marked as
 368 “uncertain” (Table 3). Fifty-six (out of 65) records are correlated with SIC when using Na⁺ flux, with an
 369 additional four sites marked as uncertain. This reflects the smaller number of flux records submitted to the
 370 database. Proportionally, more records are correlated with SIC when using flux than concentration (86 %
 371 compared to 78 %).

372

373 A total of 63 (out of 88) [Na⁺] records exhibit a significant correlation with the wind fields (v850 and u850).
 374 While an additional three records were marked as uncertain. When using Na⁺ flux 48 (out of 65) records

375 correlated with winds, with four records marked as uncertain. A higher proportion of records (74 % compared
376 with 72 %) correlated with winds when using flux.
377

378 A total of 47 (out of 88) $[Na^+]$ sites exhibit a significant correlation with geopotential height. While an
379 additional two records are marked as uncertain. The number of correlations with geopotential height is 43 (out
380 of 65) when using Na^+ flux, with an additional three sites marked as uncertain. A higher proportion of records
381 (66 % compared with 53 %) correlated with atmospheric circulation when using flux.
382



383
384 **Figure 3** – Geographical distribution of $[Na^+]$ records (left column) which exhibit a statistically significant
385 ($p > 0.05$) correlation with (a) SIC, (b) winds (v850 and u850) and (c) geopotential height (z500). Compared with
386 the geographical distribution of Na flux record (right column) which exhibit a statistically significant ($p > 0.05$)
387

388 correlation with (d) SIC, (e) winds (v850 and u850) and (f) geopotential height (z500). Pink diamonds are
389 locations with a significant correlation either positive or negative; grey diamonds are sites with no correlation,
390 open diamonds are uncertain. Dots indicate ice core locations that are in the database but either are less than 10
391 years in length (or overlap with the instrumental period) or sites which failed to generate any correlations with
392 parameters tested.

393

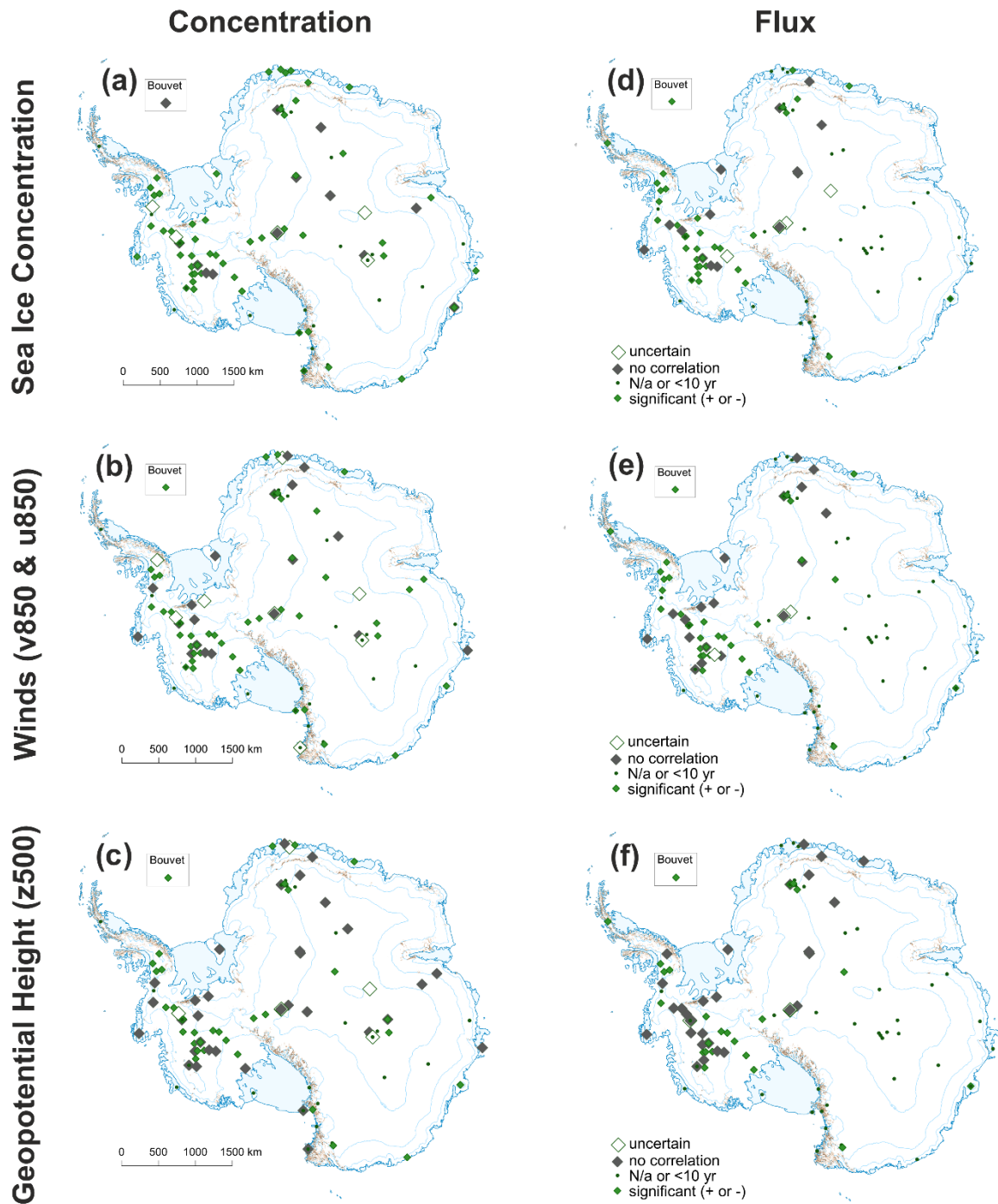
394

395 **4.3. Sulphate (concentration and flux)**

396 A total of 60 (out of 84) [SO₄²⁻] records display a correlation with SIC, with six additional records marked as
397 uncertain (Table 3). When using SO₄²⁻ flux, 40 (out of 61) records correlated with SIC, with an additional five
398 records marked as uncertain. A slightly higher proportion of records (71 % compared with 66 %) correlated with
399 SIC when using flux.

400 Fifty-four [SO₄²⁻] records (out of 84) are correlated with winds (v850 and u850), with eight additional records
401 marked as uncertain. This is compared to 39 records (out of 61), and three additional records marked as
402 uncertain, that are correlated with winds when using SO₄²⁻ flux. The proportion of records correlated with winds
403 (64 %) is the same when using either flux or concentration.

404 A total of 38 (out of 84) [SO₄²⁻] records are correlated with geopotential height, with six additional records
405 marked as uncertain. This is compared with 26 records (out of 61) when using flux, with three marked as
406 uncertain. A slightly higher proportion of records (45 % compared with 43 %) are correlated with atmospheric
407 circulation when using flux.



408

409 **Figure 4** – Geographical distribution of $[\text{SO}_4^{2-}]$ records (left column) which exhibit a statistically significant
 410 ($p > 0.05$) correlation with (a) SIC, (b) winds (v850 and u850) and (c) geopotential height (z500). Compared with
 411 the geographical distribution of SO_4^{2-} flux record (right column) which exhibit a statistically significant ($p > 0.05$)
 412 correlation with (d) SIC, (e) winds (v850 and u850) and (f) geopotential height (z500). Green diamonds are
 413 locations with a significant correlation either positive or negative; grey diamonds are sites with no correlation,
 414 open diamonds are uncertain. Dots indicate ice core locations that are in the database but either are less than 10
 415 years in length (or overlap with the instrumental period) or sites which failed to generate any correlations with
 416 parameters tested.

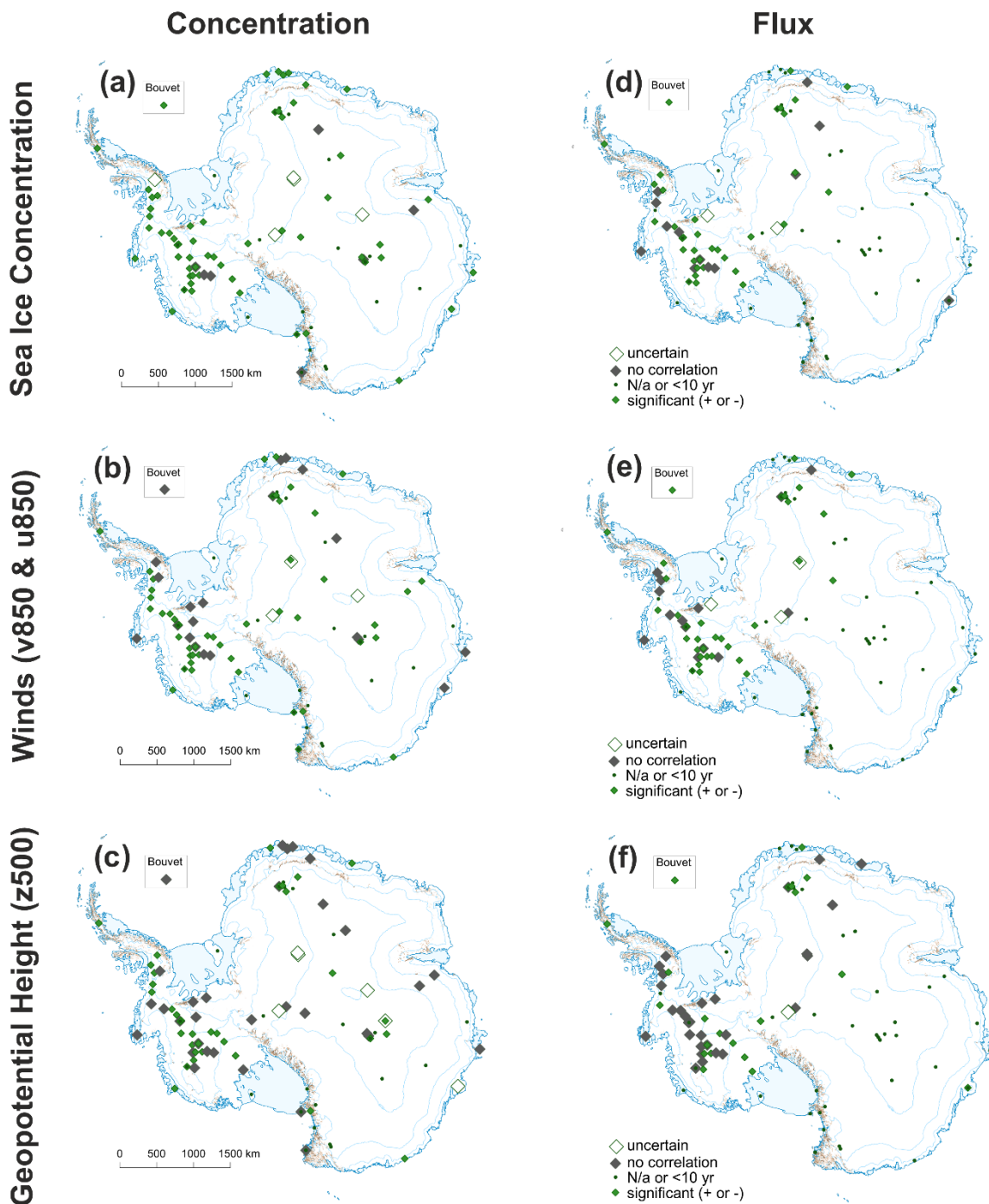
417

418 **4.4. Excess Sulphate (concentration and flux)**

419 A total of 68 (out of 81) xs [SO₄²⁻] records are correlated with SIC, with five additional records marked as
420 uncertain when using concentration (Table 3). This number drops to 42 (out of 59) when using the flux, with
421 two additional records marked as uncertain. A smaller proportion of records (71 % compared with 84 %)
422 correlated with SIC when using flux.

423 A total of 56 (out of 81) xs [SO₄²⁻] records are correlated winds (v850 and u850), with three additional records
424 marked as uncertain. The number drops to 40 (out of 59) records when using the xs SO₄²⁻ flux, with three
425 additional records marked as uncertain. A higher proportion of records (69% compared with 68 %) correlated
426 with winds when using flux.

427 A total of 40 (out of 81) xs [SO₄²⁻] concentration records are correlated with geopotential height, with an
428 additional six records marked as uncertain. The number drops to 23 (out of 59) records when using the xs SO₄²⁻
429 flux, with three additional records marked as uncertain. A smaller proportion of records (39 % compared with
430 49 %) correlated with atmospheric circulation when using flux.



431

432 **Figure 5** – Geographical distribution of xs $[\text{SO}_4^{2-}]$ records (left column) which exhibit a statistically significant
 433 ($p > 0.05$) correlation with (a) SIC, (b) winds (v850 and u850) and (c) geopotential height (z500). Compared with
 434 the geographical distribution of xs SO_4^{2-} flux record (right column) which exhibit a statistically significant
 435 ($p > 0.05$) correlation with (d) SIC, (e) winds (v850 and u850) and (f) geopotential height (z500). Green
 436 diamonds are locations with a significant correlation either positive or negative; grey diamonds are sites with no
 437 correlation, open diamonds are uncertain. Dots indicate ice core locations that are in the database but either are
 438 less than 10 years in length (or overlap with the instrumental period) or sites which failed to generate any
 439 correlations with parameters tested.

440

441 **5. Discussion**

442 **5.1. Which records are suitable for reconstructing SIC, winds and atmospheric circulation?**

443 Our findings reveal that $[\text{Na}^+]$ provides the highest number (69) of records that exhibit a significant correlation
444 with SIC. Only fractionally higher than the number of $\text{xs} [\text{SO}_4^{2-}]$ records (68) and SO_4 (60). This suggests that
445 all three records have the potential to capture changes in sea ice conditions. The full list of which sites exhibit
446 positive correlations with each parameter is shown in Supplementary Figure S2.

447 $[\text{Na}^+]$ also provides the highest number of correlations with geopotential height (47) and wind (63). However,
448 proportionally Na flux has the highest number of correlations with geopotential height and winds. While less
449 than 49% of the $[\text{SO}_4^{2-}]$ and $\text{xs} [\text{SO}_4^{2-}]$ data exhibit relationships with geopotential height, a much higher
450 percentage (64-69 %) display correlations with winds. This suggests that there is greater potential for using
451 $[\text{SO}_4^{2-}]$ and $\text{xs} [\text{SO}_4^{2-}]$ for reconstructing winds and SIC than geopotential heights. Removing the sea-salt
452 component of $[\text{SO}_4^{2-}]$ to produce $\text{xs} [\text{SO}_4^{2-}]$ improves the relationship with SIC, geopotential height and winds.

453 Most of the records from West Antarctica and the Antarctic Peninsula (both $[\text{Na}^+]$ and $[\text{SO}_4^{2-}]$) exhibit
454 correlations with SIC, geopotential height and winds. This reflects the dominance of marine air-mass incursions
455 in this region (Suzuki et al., 2013), transporting sea salt aerosols from the sea ice zone to the ice core sites. In
456 contrast, in East Antarctica the high elevation of the ice sheet (>3000 m) acts as a barrier to marine air-mass
457 transport. However, this study corroborates previous studies (e.g., (Winski et al., 2021)) suggesting that $[\text{Na}^+]$
458 and $[\text{SO}_4^{2-}]$ concentrations from ice cores in the East Antarctic plateau are significantly correlated with SIC and
459 atmospheric circulation.

460 Converting the records to flux drastically reduces the geographical coverage. In most cases this is due to the lack
461 of available snow accumulation records from central Antarctica needed to calculate the flux. However, our study
462 demonstrates that converting $[\text{Na}^+]$ to flux increases the relative proportion of records that exhibit a significant
463 correlation with SIC, geopotential height and winds. The opposite is true for $[\text{SO}_4^{2-}]$ and $\text{xs} [\text{SO}_4^{2-}]$, which
464 results in a lower proportion of records correlating with SIC after converting to flux. This may suggest a
465 dominance of wet deposition of $[\text{Na}^+]$ and dry deposition of $[\text{SO}_4^{2-}]$. However, a detailed evaluation of the
466 relationships between ion concentration and snow accumulation is needed to address this fully.

467 Overall, the records of $[\text{Na}^+]$ exhibit the highest number of correlations with the climatic variables considered
468 (179 out of 264), followed by $\text{xs} [\text{SO}_4^{2-}]$ (164 out of 243) and $[\text{SO}_4^{2-}]$ (152 out of 252).

469 5.2. Potential limitations

470 There are limitations to this assessment, which is intended as a first pass filter to highlight the potential future
471 use of the data. In particular, the numbers only relate to records that span or have at least 10-years of data that
472 overlap with the instrumental period. This is defined as the period from 1979-2019 and accounts for 88% of the
473 records (438 out of 499 records submitted). Thus, relationships may exist for shorter records or records drilled
474 prior to 1979, however, it is not possible to verify this under the criteria defined here. Another caveat is that
475 correlations have only been conducted with a single sea ice (NSIDC) and reanalysis (ERA-5) product, and
476 results may vary with different datasets. Results may also be impacted by the different timespans used. For
477 example, it was not possible to select the same reference period to run all correlations, because record lengths
478 and top ages (date the core was drilled) vary considerably. Thus, the assumed stationarity in the source and
479 transport routes may not be appropriate.

480 We also note that almost 8% of the records have been classified as “uncertain”. In some cases, significant
481 correlations were evident in the plots, but they were difficult to explain (Fig. 2c). For example, Law Dome
482 generates several regions of significant correlations across multiple sectors, however not in the ocean adjacent to
483 the site. This may indicate long-term transport or the influence of large-scale atmospheric circulation (e.g.,
484 SAM, Indian Ocean Dipole, Atlantic Multidecadal Oscillation). However, in this first pass filter we only
485 included sites where a clear mechanism was evident.

486

487 6. Data availability

488 This data descriptor presents version 1.0.0 of the CLIVASH2k Antarctic ice core chemistry database PAGES
489 CLIVASH2k database (Thomas et al., 2022). The database can be accessed via the UK Polar Data Centre.
490 NERC EDS UK Polar Data Centre. <https://doi.org/10.5285/9E0ED16E-F2AB-4372-8DF3-FDE7E388C9A7>

491
492 **7. Conclusions.**

493 The CLIVASH2k database is the first compilation of an Antarctic continental-scale database of chemical
494 records in ice cores spanning the past 2000 years. This study is the first phase of the project, the goal of which
495 was to compile and publish the records. We have provided all available $[\text{Na}^+]$ and $[\text{SO}_4^{2-}]$ records submitted by
496 the community. The records are all available as annual averages, included as both concentration and flux (where
497 available). An additional parameter, $x_s [\text{SO}_4^{2-}]$ has also been calculated where possible.

498 To facilitate future data interpretation, we have run spatial correlations for all the records. The aim of this
499 analysis is to identify sites which exhibit a statistically significant relationship with sea ice concentration (SIC)
500 and atmospheric circulation (500-hPa geopotential heights) or winds (v850 and u850). This is intended as a first
501 filter to identify potential records that could be used in future proxy reconstructions.

502 This first pass filter demonstrates that when considering the species separately, 335 individual records exhibit
503 statistically significant correlations with SIC that have been verified by a team of experts. A recent compilation
504 of available ice core derived sea ice reconstructions, based on a range of proxy data, identified only 17
505 individual sites which have been used to reconstruct sea ice (Thomas et al., 2019). Thus, this data compilation
506 represents a significant improvement on existing published or available data.

507 For researchers interested in reconstructing winds or atmospheric circulation the CLIVASH2k database contains
508 a total of 300 records that are significantly correlated with the wind fields (v850 and u850) and 217 records that
509 are significantly correlated with geopotential height (500 hPa). The Na^+ flux exhibits the greatest proportion of
510 records that correlate with sea ice, atmospheric circulation, and winds. Therefore, among the ice-core chemical
511 species considered in our analysis, we propose Na^+ flux as the best candidate for reconstructing all three climatic
512 components.

513 Future work will focus on using this database to:

- 514 1) Investigate the deposition of $[\text{Na}^+]$ and $[\text{SO}_4^{2-}]$ over decadal to centennial timescales.
- 515 2) Provide a reconstruction of sea ice distribution or atmospheric circulation spanning the past 2000 years.
- 516 3) Evaluate the skill of chemical transport models to capture observed deposition of $[\text{Na}^+]$ and $[\text{SO}_4^{2-}]$.
- 517 4) Combine the information in this new database with the database of snow accumulation (Thomas et al.,
518 2017) and isotopic content (Stenni et al., 2017) to obtain a comprehensive view of Antarctic climate
519 variations over the past 2000 years.

520 This is not an exhaustive list, and we encourage the community to engage with the CLIVASH2k working group
521 and make use of the database.

522

523 **Author contributions**

524 ET and HG conceived the idea. ET & DV initiated the data call and coordinated the project. ET wrote the paper
525 with contributions from the core writing group. The core writing group (DV, ACFK, DE, HG, DW, VHLW,
526 DD, DU, TV), contributed to the paper writing and discussions. The data interpretation team (ET, DV, ACFK,
527 DW, VHLW, DD, NC, DU, TV, DT, MMG, MS) quality checked the data, evaluated the age-scales, and
528 interpreted the spatial correlation plots. NANB, AH, CML, JRM, YM, KT, HM, YN, FS, JCS, MS, RT, SW,
529 CX, JY, TVK, AAE, LPG and EMT all provided unpublished data. DE wrote the code for the data interpretation
530 plots. DV & LT compiled the figures. All authors read and commented on the manuscript.

531 The following researchers contributed published data to this database. Yoshiyuki Fujii, Lenneke Jong, Elisabeth
532 Isaksson, Filipe G. L. Lindau, Andrew Moy, Rachael Rhodes. We thank the many other researchers who have
533 already made their data available on public data repositories.

534 **Competing interests**

535 The authors declare no competing conflict of interest.

536 **Acknowledgements**

537 CLIVASH2k is a contribution of Phase 3 of the PAGES 2k network. DT was funded as part of the PAGES Data
538 Stewardship scholarship awarded to ET. This financial support comes from the Chinese Academy of Sciences
539 (CAS) and the Swiss Academy of Sciences (SCNAT). We thank the PAGES office for their support and the
540 temporary data storage during the compilation of this database. We thank editor Petra Heil and two anonymous
541 reviewers for their constructive review and recommendations.

542 References

- 543 Arienzo, M. M., McConnell, J. R., Chellman, N., and Kipfstuhl, S.: Method for Correcting Continuous Ice-Core
544 Elemental Measurements for Under-Recovery, *Environmental Science & Technology*, 53, 5887-5894,
545 10.1021/acs.est.9b00199, 2019.
- 546 Barnes, I., Hjorth, J., and Mihalopoulos, N.: Dimethyl Sulfide and Dimethyl Sulfoxide and Their Oxidation in
547 the Atmosphere, *Chemical Reviews*, 106, 940-975, 10.1021/cr020529+, 2006.
- 548 Brean, J., Dall'Osto, M., Simó, R., Shi, Z., Beddows, D. C. S., and Harrison, R. M.: Open ocean and coastal
549 new particle formation from sulfuric acid and amines around the Antarctic Peninsula, *Nature*
550 *Geoscience*, 14, 383-388, 10.1038/s41561-021-00751-y, 2021.
- 551 Büntgen, U., Wacker, L., Galván, J. D., Arnold, S., Arseneault, D., Baillie, M., Beer, J., Bernabei, M., Bleicher,
552 N., Boswijk, G., Bräuning, A., Carrer, M., Ljungqvist, F. C., Cherubini, P., Christl, M., Christie, D. A.,
553 Clark, P. W., Cook, E. R., D'Arrigo, R., Davi, N., Eggertsson, Ó., Esper, J., Fowler, A. M., Gedalof, Z.
554 e., Gennaretti, F., Griesinger, J., Grissino-Mayer, H., Grudd, H., Gunnarson, B. E., Hantemirov, R.,
555 Herzig, F., Hessel, A., Heussner, K.-U., Jull, A. J. T., Kukarskih, V., Kirilyanov, A., Kolář, T., Krusic,
556 P. J., Kyncl, T., Lara, A., LeQuesne, C., Linderholm, H. W., Loader, N. J., Luckman, B., Miyake, F.,
557 Myglan, V. S., Nicolussi, K., Oppenheimer, C., Palmer, J., Panyushkina, I., Pederson, N., Rybníček,
558 M., Schweingruber, F. H., Seim, A., Sigl, M., Churakova, O., Speer, J. H., Synal, H.-A., Tegel, W.,
559 Treydte, K., Villalba, R., Wiles, G., Wilson, R., Winship, L. J., Wunder, J., Yang, B., and Young, G. H.
560 F.: Tree rings reveal globally coherent signature of cosmogenic radiocarbon events in 774 and 993 CE,
561 *Nature Communications*, 9, 3605, 10.1038/s41467-018-06036-0, 2018.
- 562 Cavalieri, D. J., Gloersen, P., Parkinson, C. L., Comiso, J. C., and Zwally, H. J.: Observed hemispheric
563 asymmetry in global sea ice changes, *Science*, 278, 1104-1106, 1997.
- 564 Cole-Dai, J., Ferris, D. G., Kennedy, J. A., Sigl, M., McConnell, J. R., Fudge, T. J., Geng, L., Maselli, O. J.,
565 Taylor, K. C., and Souney, J. M.: Comprehensive Record of Volcanic Eruptions in the Holocene
566 (11,000 years) From the WAIS Divide, Antarctica Ice Core, *Journal of Geophysical Research:*
567 *Atmospheres*, 126, e2020JD032855, <https://doi.org/10.1029/2020JD032855>, 2021.
- 568 Dalaiden, Q., Goosse, H., Rezsöhazy, J., and Thomas, E. R.: Reconstructing atmospheric circulation and sea-ice
569 extent in the West Antarctic over the past 200 years using data assimilation, *Climate Dynamics*,
570 10.1007/s00382-021-05879-6, 2021.
- 571 Delmas, R., Briat, M., and Legrand, M.: Chemistry of south polar snow, *Journal of Geophysical Research:*
572 *Oceans*, 87, 4314-4318, <https://doi.org/10.1029/JC087iC06p04314>, 1982.
- 573 Dixon, D., Mayewski, P. A., Kaspari, S., Sneed, S., and Handley, M.: A 200 year sub-annual record of sulfate in
574 West Antarctica, from 16 ice cores, *Annals of Glaciology*, 39, 545-556,
575 10.3189/172756404781814113, 2004.
- 576 Ekaykin, A. A., Kozachek, A. V., Lipenkov, V. Y., and Shibaev, Y. A.: Multiple climate shifts in the Southern
577 Hemisphere over the past three centuries based on central Antarctic snow pits and core studies, *Annals*
578 *of Glaciology*, 55, 259-266, 10.3189/2014Aog66A189, 2014.
- 579 Emanuelsson, B. D., Thomas, E. R., Tetzner, D. R., Humby, J. D., and Vladimirova, D. O.: Ice Core
580 Chronologies from the Antarctic Peninsula: The Palmer, Jurassic, and Rendezvous Age-Scales,
581 *Geosciences*, 12, 87, 2022.
- 582 Fogt, R. L., Sleinkofer, A. M., Raphael, M. N., and Handcock, M. S.: A regime shift in seasonal total Antarctic
583 sea ice extent in the twentieth century, *Nature Climate Change*, 12, 54-62, 10.1038/s41558-021-01254-
584 9, 2022.
- 585 Frey, M. M., Norris, S. J., Brooks, I. M., Anderson, P. S., Nishimura, K., Yang, X., Jones, A. E., Nerentorp
586 Mastromonaco, M. G., Jones, D. H., and Wolff, E. W.: First direct observation of sea salt aerosol
587 production from blowing snow above sea ice, *Atmospheric Chemistry and Physics*, 20, 2549-2578,
588 2020.
- 589 Gondwe, M., Krol, M., Gieskes, W., Klaassen, W., and de Baar, H.: The contribution of ocean-leaving DMS to
590 the global atmospheric burdens of DMS, MSA, SO₂, and NSS SO₄⁼, *Global Biogeochemical Cycles*,
591 17, <https://doi.org/10.1029/2002GB001937>, 2003.
- 592 Grieman, M. M., Hoffmann, H. M., Humby, J. D., Mulvaney, R., Nehrbass-Ahles, C., Rix, J., Thomas, E. R.,
593 Tuckwell, R., and Wolff, E. W.: Continuous flow analysis methods for sodium, magnesium and

594 calcium detection in the Skytrain ice core, *Journal of Glaciology*, 68, 90-100, 10.1017/jog.2021.75,
595 2022.

596 Hersbach, H., Bell, B., Berrisford, P., Hirahara, S., Horányi, A., Muñoz-Sabater, J., Nicolas, J., Peubey, C.,
597 Radu, R., and Schepers, D.: The ERA5 global reanalysis, *Quarterly Journal of the Royal*
598 *Meteorological Society*, 146, 1999-2049, 2020.

599 Holland, H. D.: *The chemistry of the atmosphere and oceans*, 1978.

600 Huang, J. and Jaeglé, L.: Wintertime enhancements of sea salt aerosol in polar regions consistent with a sea ice
601 source from blowing snow, *Atmos. Chem. Phys.*, 17, 3699-3712, 10.5194/acp-17-3699-2017, 2017.

602 Jones, J. M., Gille, S. T., Goosse, H., Abram, N. J., Canziani, P. O., Charman, D. J., Clem, K. R., Crosta, X., de
603 Lavergne, C., Eisenman, I., England, M. H., Fogt, R. L., Frankcombe, L. M., Marshall, G. J., Masson-
604 Delmotte, V., Morrison, A. K., Orsi, A. J., Raphael, M. N., Renwick, J. A., Schneider, D. P., Simpkins,
605 G. R., Steig, E. J., Stenni, B., Swingedouw, D., and Vance, T. R.: Assessing recent trends in high-
606 latitude Southern Hemisphere surface climate, *Nature Climate Change*, 6, 917-926,
607 10.1038/nclimate3103, 2016.

608 Jungclaus, J. H., Bard, E., Baroni, M., Braconnot, P., Cao, J., Chini, L. P., Egorova, T., Evans, M., González-
609 Rouco, J. F., Goosse, H., Hurrell, G. C., Joos, F., Kaplan, J. O., Khodri, M., Klein Goldewijk, K.,
610 Krivova, N., LeGrande, A. N., Lorenz, S. J., Luterbacher, J., Man, W., Maycock, A. C., Meinshausen,
611 M., Moberg, A., Muscheler, R., Nehrbass-Ahles, C., Otto-Bliesner, B. L., Phipps, S. J., Pongratz, J.,
612 Rozanov, E., Schmidt, G. A., Schmidt, H., Schmutz, W., Schurer, A., Shapiro, A. I., Sigl, M.,
613 Smerdon, J. E., Solanki, S. K., Timmreck, C., Toohey, M., Usoskin, I. G., Wagner, S., Wu, C. J., Yeo,
614 K. L., Zanchettin, D., Zhang, Q., and Zorita, E.: The PMIP4 contribution to CMIP6 – Part 3: The last
615 millennium, scientific objective, and experimental design for the PMIP4 past1000 simulations, *Geosci.*
616 *Model Dev.*, 10, 4005-4033, 10.5194/gmd-10-4005-2017, 2017.

617 Kaufman, D., McKay, N., Routson, C., Erb, M., Dätwyler, C., Sommer, P. S., Heiri, O., and Davis, B.:
618 Holocene global mean surface temperature, a multi-method reconstruction approach, *Scientific Data*, 7,
619 201, 10.1038/s41597-020-0530-7, 2020.

620 Konecny, B. L., McKay, N. P., Churakova, O. V., Comas-Bru, L., Dassié, E. P., DeLong, K. L., Falster, G. M.,
621 Fischer, M. J., Jones, M. D., Jonkers, L., Kaufman, D. S., Leduc, G., Managave, S. R., Martrat, B.,
622 Opel, T., Orsi, A. J., Partin, J. W., Sayani, H. R., Thomas, E. K., Thompson, D. M., Tyler, J. J., Abram,
623 N. J., Atwood, A. R., Cartapanis, O., Conroy, J. L., Curran, M. A., Dee, S. G., Deininger, M., Divine,
624 D. V., Kern, Z., Porter, T. J., Stevenson, S. L., von Gunten, L., and Iso2k Project, M.: The Iso2k
625 database: a global compilation of paleo- $\delta^{18}\text{O}$ and $\delta^2\text{H}$ records to aid understanding of Common Era
626 climate, *Earth Syst. Sci. Data*, 12, 2261-2288, 10.5194/essd-12-2261-2020, 2020.

627 Legrand, M. and Mayewski, P.: Glaciochemistry of polar ice cores: A review, *Reviews of Geophysics*, 35, 219-
628 243, <https://doi.org/10.1029/96RG03527>, 1997.

629 Legrand, M., Feniet-Saigne, C., Saltzman, E. S., and Germain, C.: Spatial and temporal variations of
630 methanesulfonic acid and non sea salt sulfate in Antarctic ice, *Journal of Atmospheric Chemistry*, 14,
631 245-260, 10.1007/BF00115237, 1992.

632 Lide, D.: *CRC Handbook of Chemistry and Physics*, Internet Version 2005 CRC Press, Boca Raton, FL, 2005.

633 Livezey, R. E. and Chen, W.: Statistical field significance and its determination by Monte Carlo techniques,
634 *Mon. Wea. Rev.*, 111, 46-59, 1983.

635 Mayewski, P. A., Carleton, A. M., Birkel, S. D., Dixon, D., Kurbatov, A. V., Korotkikh, E., McConnell, J.,
636 Curran, M., Cole-Dai, J., Jiang, S., Plummer, C., Vance, T., Maasch, K. A., Sneed, S. B., and Handley,
637 M.: Ice core and climate reanalysis analogs to predict Antarctic and Southern Hemisphere climate
638 changes, *Quaternary Science Reviews*, 155, 50-66, <https://doi.org/10.1016/j.quascirev.2016.11.017>,
639 2017.

640 McCoy, D. T., Burrows, S. M., Wood, R., Grosvenor, D. P., Elliott, S. M., Ma, P.-L., Rasch, P. J., and
641 Hartmann, D. L.: Natural aerosols explain seasonal and spatial patterns of Southern Ocean cloud
642 albedo, *Science Advances*, 1, e1500157, doi:10.1126/sciadv.1500157, 2015.

643 McGregor, H. V., Evans, M. N., Goosse, H., Leduc, G., Martrat, B., Addison, J. A., Mortyn, P. G., Oppo, D.
644 W., Seidenkrantz, M.-S., Sicre, M.-A., Phipps, S. J., Selvaraj, K., Thirumalai, K., Filipsson, H. L., and
645 Ersek, V.: Robust global ocean cooling trend for the pre-industrial Common Era, *Nature Geoscience*, 8,
646 671-677, 10.1038/ngeo2510, 2015.

647 McKay, N. P. and Kaufman, D. S.: An extended Arctic proxy temperature database for the past 2,000 years,
648 *Scientific Data*, 1, 140026, 10.1038/sdata.2014.26, 2014.

649 Medley, B. and Thomas, E. R.: Increased snowfall over the Antarctic Ice Sheet mitigated twentieth-century sea-
650 level rise, *Nature Climate Change*, 9, 34-39, 10.1038/s41558-018-0356-x, 2019.

651 Meehl, G. A., Arblaster, J. M., Bitz, C. M., Chung, C. T. Y., and Teng, H.: Antarctic sea-ice expansion between
652 2000 and 2014 driven by tropical Pacific decadal climate variability, *Nature Geoscience*, 9, 590-595,
653 10.1038/ngeo2751, 2016.

654 Minikin, A., Wagenbach, D., Graf, W., and Kipfstuhl, J.: Spatial and seasonal variations of the snow chemistry
655 at the central Filchner-Ronne Ice Shelf, Antarctica, *Annals of Glaciology*, 20, 283-290, 1994.

656 Münch, T. and Laepple, T.: What climate signal is contained in decadal- to centennial-scale isotope variations
657 from Antarctic ice cores?, *Clim. Past*, 14, 2053-2070, 10.5194/cp-14-2053-2018, 2018.

658 O'Brien, S. R., Mayewski, P. A., Meeker, L. D., Meese, D. A., Twickler, M. S., and Whitlow, S. I.: Complexity
659 of Holocene Climate as Reconstructed from a Greenland Ice Core, *Science*, 270, 1962-1964,
660 doi:10.1126/science.270.5244.1962, 1995.

661 Plummer, C. T., Curran, M. A. J., van Ommen, T. D., Rasmussen, S. O., Moy, A. D., Vance, T. R., Clausen, H.
662 B., Vinther, B. M., and Mayewski, P. A.: An independently dated 2000-yr volcanic record from Law
663 Dome, East Antarctica, including a new perspective on the dating of the 1450s CE eruption of Kuwae,
664 Vanuatu, *Clim. Past*, 8, 1929-1940, 10.5194/cp-8-1929-2012, 2012.

665 Rankin, A. M., Auld, V., and Wolff, E. W.: Frost flowers as a source of fractionated sea salt aerosol in the polar
666 regions, *Geophysical Research Letters*, 27, 3469-3472, 10.1029/2000gl011771, 2000.

667 Rankin, A. M., Wolff, E. W., and Martin, S.: Frost flowers: Implications for tropospheric chemistry and ice core
668 interpretation, *Journal of Geophysical Research: Atmospheres*, 107, AAC 4-1-AAC 4-15,
669 10.1029/2002jd002492, 2002.

670 Ren, J., Li, C., Hou, S., Xiao, C., Qin, D., Li, Y., and Ding, M.: A 2680 year volcanic record from the DT-401
671 East Antarctic ice core, *Journal of Geophysical Research: Atmospheres*, 115,
672 <https://doi.org/10.1029/2009JD012892>, 2010.

673 Rhodes, R. H., Yang, X., and Wolff, E. W.: Sea Ice Versus Storms: What Controls Sea Salt in Arctic Ice Cores?,
674 *Geophysical Research Letters*, 45, 5572-5580, 10.1029/2018gl077403, 2018.

675 Roach, L. A., Dörr, J., Holmes, C. R., Massonnet, F., Blockley, E. W., Notz, D., Rackow, T., Raphael, M. N.,
676 O'Farrell, S. P., Bailey, D. A., and Bitz, C. M.: Antarctic Sea Ice Area in CMIP6, *Geophysical
677 Research Letters*, 47, e2019GL086729, <https://doi.org/10.1029/2019GL086729>, 2020.

678 Saltzman, E. S., Dioumaeva, I., and Finley, B. D.: Glacial/interglacial variations in methanesulfonate (MSA) in
679 the Siple Dome ice core, West Antarctica, *Geophysical Research Letters*, 33,
680 <https://doi.org/10.1029/2005GL025629>, 2006.

681 Severi, M., Becagli, S., Caiazzo, L., Ciardini, V., Colizza, E., Giardi, F., Mezgec, K., Scarchilli, C., Stenni, B.,
682 Thomas, E. R., Traversi, R., and Udisti, R.: Sea salt sodium record from Talos Dome (East Antarctica)
683 as a potential proxy of the Antarctic past sea ice extent, *Chemosphere*, 177, 266-274,
684 <https://doi.org/10.1016/j.chemosphere.2017.03.025>, 2017.

685 Sigl, M., McConnell, J. R., Toohey, M., Curran, M., Das, S. B., Edwards, R., Isaksson, E., Kawamura, K.,
686 Kipfstuhl, S., Krüger, K., Layman, L., Maselli, O. J., Motizuki, Y., Motoyama, H., Pasteris, D. R., and
687 Severi, M.: Insights from Antarctica on volcanic forcing during the Common Era, *Nature Climate
688 Change*, 4, 693-697, 10.1038/nclimate2293, 2014.

689 Sigl, M., Winstrup, M., McConnell, J. R., Welten, K. C., Plunkett, G., Ludlow, F., Büntgen, U., Caffee, M.,
690 Chellman, N., Dahl-Jensen, D., Fischer, H., Kipfstuhl, S., Kostick, C., Maselli, O. J., Mekhaldi, F.,
691 Mulvaney, R., Muscheler, R., Pasteris, D. R., Pilcher, J. R., Salzer, M., Schüpbach, S., Steffensen, J. P.,
692 Vinther, B. M., and Woodruff, T. E.: Timing and climate forcing of volcanic eruptions for the past
693 2,500 years, *Nature*, 523, 543-549, 10.1038/nature14565, 2015.

694 Sigl, M., Fudge, T. J., Winstrup, M., Cole-Dai, J., Ferris, D., McConnell, J. R., Taylor, K. C., Welten, K. C.,
695 Woodruff, T. E., Adolphi, F., Bisiaux, M., Brook, E. J., Buizert, C., Caffee, M. W., Dunbar, N. W.,
696 Edwards, R., Geng, L., Iverson, N., Koffman, B., Layman, L., Maselli, O. J., McGwire, K., Muscheler,
697 R., Nishiizumi, K., Pasteris, D. R., Rhodes, R. H., and Sowers, T. A.: The WAIS Divide deep ice core
698 WD2014 chronology – Part 2: Annual-layer counting (0–31 ka BP), *Clim. Past*, 12, 769-786,
699 10.5194/cp-12-769-2016, 2016.

700 Sneed, S. B., Mayewski, P. A., and Dixon, D. A.: An emerging technique: multi-ice-core multi-parameter
701 correlations with Antarctic sea-ice extent, *Annals of Glaciology*, 52, 347-354,
702 10.3189/172756411795931822, 2011.

703 Stenni, B., Curran, M. A. J., Abram, N. J., Orsi, A., Goursaud, S., Masson-Delmotte, V., Neukom, R., Goosse,
704 H., Divine, D., van Ommen, T., Steig, E. J., Dixon, D. A., Thomas, E. R., Bertler, N. A. N., Isaksson,
705 E., Ekaykin, A., Werner, M., and Frezzotti, M.: Antarctic climate variability on regional and
706 continental scales over the last 2000 years, *Clim. Past*, 13, 1609-1634, 10.5194/cp-13-1609-2017,
707 2017.

708 Suzuki, K., Yamanouchi, T., Kawamura, K., and Motoyama, H.: The spatial and seasonal distributions of air-
709 transport origins to the Antarctic based on 5-day backward trajectory analysis, *Polar Science*, 7, 205-
710 213, <https://doi.org/10.1016/j.polar.2013.08.001>, 2013.

711 Tetzner, D. R., Thomas, E. R., and Allen, C. S.: Marine diatoms in ice cores from the Antarctic Peninsula and
712 Ellsworth Land, Antarctica – species diversity and regional variability, *The Cryosphere Discuss.*, 2021,
713 1-32, 10.5194/tc-2021-160, 2021a.

714 Tetzner, D. R., Thomas, E. R., Allen, C. S., and Piermattei, A.: Evidence of Recent Active Volcanism in the
715 Balleny Islands (Antarctica) From Ice Core Records, *Journal of Geophysical Research: Atmospheres*,
716 126, e2021JD035095, <https://doi.org/10.1029/2021JD035095>, 2021b.

717 Thomas, E. R.: Antarctic regional snow accumulation composites over the past 1000 years" v2 , [dataset],
718 doi:10.5285/cc1d42de-dfe6-40aa-a1a6-d45cb2fc8293, 2017.

719 Thomas, E. R., Marshall, G. J., and McConnell, J. R.: A doubling in snow accumulation in the western Antarctic
720 Peninsula since 1850, *Geophysical Research Letters*, 35, <https://doi.org/10.1029/2007GL032529>, 2008.

721 Thomas, E. R., Vladimirova, D., and Tetzner, D. R.: CLIVASH2k Antarctic ice core chemistry database
722 (Version 1.0) [Data set]. [dataset], [https://doi.org/10.5285/9E0ED16E-F2AB-4372-8DF3-
723 FDE7E388C9A7](https://doi.org/10.5285/9E0ED16E-F2AB-4372-8DF3-FDE7E388C9A7), 2022.

724 Thomas, E. R., Dennis, P. F., Bracegirdle, T. J., and Franzke, C.: Ice core evidence for significant 100-year
725 regional warming on the Antarctic Peninsula, *Geophysical Research Letters*, 36,
726 <https://doi.org/10.1029/2009GL040104>, 2009.

727 Thomas, E. R., Allen, C. S., Etourneau, J., King, A. C. F., Severi, M., Winton, V. H. L., Mueller, J., Crosta, X.,
728 and Peck, V. L.: Antarctic Sea Ice Proxies from Marine and Ice Core Archives Suitable for
729 Reconstructing Sea Ice over the Past 2000 Years, *Geosciences*, 9, 506, 2019.

730 Thomas, E. R., van Wessem, J. M., Roberts, J., Isaksson, E., Schlosser, E., Fudge, T. J., Vallelonga, P., Medley,
731 B., Lenaerts, J., Bertler, N., van den Broeke, M. R., Dixon, D. A., Frezzotti, M., Stenni, B., Curran, M.,
732 and Ekaykin, A. A.: Regional Antarctic snow accumulation over the past 1000 years, *Clim. Past*, 13,
733 1491-1513, 10.5194/cp-13-1491-2017, 2017.

734 Tierney, J. E., Abram, N. J., Anchukaitis, K. J., Evans, M. N., Giry, C., Kilbourne, K. H., Saenger, C. P., Wu, H.
735 C., and Zinke, J.: Tropical sea surface temperatures for the past four centuries reconstructed from coral
736 archives, *Paleoceanography*, 30, 226-252, <https://doi.org/10.1002/2014PA002717>, 2015.

737 Turner, J., Comiso, J. C., Marshall, G. J., Lachlan-Cope, T. A., Bracegirdle, T., Maksym, T., Meredith, M. P.,
738 Wang, Z., and Orr, A.: Non-annular atmospheric circulation change induced by stratospheric ozone
739 depletion and its role in the recent increase of Antarctic sea ice extent, *Geophysical Research Letters*,
740 36, 10.1029/2009gl037524, 2009.

741 Turner, J., Holmes, C., Caton Harrison, T., Phillips, T., Jena, B., Reeves-Francois, T., Fogt, R., Thomas, E. R.,
742 and Bajish, C. C.: Record Low Antarctic Sea Ice Cover in February 2022, *Geophysical Research
743 Letters*, 49, e2022GL098904, <https://doi.org/10.1029/2022GL098904>, 2022.

744 Turner, J., Lu, H., White, I., King, J. C., Phillips, T., Hosking, J. S., Bracegirdle, T. J., Marshall, G. J.,
745 Mulvaney, R., and Deb, P.: Absence of 21st century warming on Antarctic Peninsula consistent with
746 natural variability, *Nature*, 535, 411-415, 10.1038/nature18645, 2016.

747 WAIS_Divide_Project_Members.: Onset of deglacial warming in West Antarctica driven by local orbital
748 forcing, *Nature*, 500, 440-444, 10.1038/nature12376, 2013.

749 WAISDivideProjectMembers, Fudge, T. J., Steig, E. J., Markle, B. R., Schoenemann, S. W., Ding, Q., Taylor,
750 K. C., McConnell, J. R., Brook, E. J., Sowers, T., White, J. W. C., Alley, R. B., Cheng, H., Clow, G.
751 D., Cole-Dai, J., Conway, H., Cuffey, K. M., Edwards, J. S., Lawrence Edwards, R., Edwards, R.,
752 Fegyveresi, J. M., Ferris, D., Fitzpatrick, J. J., Johnson, J., Hargreaves, G., Lee, J. E., Maselli, O. J.,
753 Mason, W., McGwire, K. C., Mitchell, L. E., Mortensen, N., Neff, P., Orsi, A. J., Popp, T. J., Schauer,
754 A. J., Severinghaus, J. P., Sigl, M., Spencer, M. K., Vaughn, B. H., Voigt, D. E., Waddington, E. D.,
755 Wang, X., and Wong, G. J.: Onset of deglacial warming in West Antarctica driven by local orbital
756 forcing, *Nature*, 500, 440-444, 10.1038/nature12376, 2013.

757 Winski, D. A., Osterberg, E. C., Kreutz, K. J., Ferris, D. G., Cole-Dai, J., Thundercloud, Z., Huang, J.,
758 Alexander, B., Jaeglé, L., Kennedy, J. A., Larrick, C., Kahle, E. C., Steig, E. J., and Jones, T. R.:
759 Seasonally Resolved Holocene Sea Ice Variability Inferred From South Pole Ice Core Chemistry,
760 *Geophysical Research Letters*, 48, e2020GL091602, <https://doi.org/10.1029/2020GL091602>, 2021.

761 Wolff, E. W.: Chemical signals of past climate and environment from polar ice cores and firm air, *Chemical
762 Society Reviews*, 41, 6247-6258, 10.1039/C2CS35227C, 2012.

763 Wolff, E. W., Fischer, H., Fundel, F., Ruth, U., Twarloh, B., Littot, G. C., Mulvaney, R., Rothlisberger, R., de
764 Angelis, M., Boutron, C. F., Hansson, M., Jonsell, U., Hutterli, M. A., Lambert, F., Kaufmann, P.,
765 Stauffer, B., Stocker, T. F., Steffensen, J. P., Bigler, M., Siggaard-Andersen, M. L., Udisti, R., Becagli,
766 S., Castellano, E., Severi, M., Wagenbach, D., Barbante, C., Gabrielli, P., and Gaspari, V.: Southern
767 Ocean sea-ice extent, productivity and iron flux over the past eight glacial cycles, *Nature*, 440, 491-
768 496, 2006.

769 Zwally, H. J., Comiso, J. C., Parkinson, C. L., Cavalieri, D. J., and Gloersen, P.: Variability of Antarctic sea ice
770 1979–1998, *Journal of Geophysical Research: Oceans*, 107, 9-1-9-19, 10.1029/2000jc000733, 2002.

771